Inner-shell photoionization-pumped x-ray lasers. Boron*

T. S. Axelrod
Lawrence Livermore Laboratory, Livermore, California 94550
(Received 13 September 1976)

A method of producing inversion by multistage x-ray pumping of low-Z elements is described. A detailed numerical model of the physical processes involved has been created and applied to boron. It is shown that significant inversion of the 255-eV $K\alpha$ transition of hydrogen-like boron may be produced with an optical pump laser, producing on the order of 5×10^{16} W/cm^2. Demonstration of x-ray lasing will require a pump laser power of at least 20 TW and the solution of several technological problems which are briefly discussed.

I. INTRODUCTION

A previous paper[1] has discussed the possibilities for producing x-ray lasing by illumination of a moderate-Z material with an intense flash of x-rays. Sulfur was considered in detail since it had previously[2] been identified as the most promising material for this approach. It was concluded that the necessary rise-time and focal-spot-size requirements for the x-ray pump source are unattainable with current technology.

The present paper analyzes a similar approach applied to a low-Z material with substantially lower transition energy. The method of producing inversion in this case is conceptually quite different from the moderate-Z case considered previously, in that it relies on a chain of inner-shell photoionization and Auger processes which results predominantly in excited heliumlike and hydrogenlike ions which form the lasing species.[3] The basic idea is made clear if one considers an initially neutral atom in the configuration $1s^2 2s^2 2p^n$ exposed to a flux of x rays with photon energy sufficient to ionize the K shell. Neglecting for the moment all processes but K shell photoionization and KLL Auger decay, it is clear that each K-shell photoionization will be followed by KLL Auger decay until the L shell is occupied by either zero or one electron, after which only photoionization can occur. If Z is odd, the states $1s^2 2p$ and $1s^2 2s$ will be populated after the last Auger decay, while if Z is even the state $1s^2$ will be populated. Clearly, if Z is odd, subsequent photoionizations will populate the states $1s2p$ and $2p$, which are suitable upper states for a self-terminating laser, while the case of even Z is of no interest.

In the actual system, a very great variety of physical processes occur which greatly complicate the above picture, resulting in a complex network of interconnected states instead of a single chain. To investigate this system in detail, a computer model which includes all known relevant processes has been created and applied to boron, the lowest-Z element of interest for this approach, which has a hydrogenic transition energy of 255 eV. In Sec. II the details of the physical model are described, while Sec. III describes the results of the model, and Sec. IV discusses the design of a practical x ray laser.

II. MODELING OF PHYSICAL PROCESSES

A. Photoionization

Calculation of the photoionization rates is straightforward. Screened hydrogenic cross sections have been used for all but neutral and singly ionized boron, for which Hartree-Fock cross sections are required for sufficient accuracy. The time-dependent photon flux is supplied to the code for typically fifty photon energy groups, which are selected to give good spectral resolution near absorption edges. The photoionization rate is determined for each ion by numerically integrating the product of the appropriate cross section and the photon flux over photon energy using power-law interpolation between groups.

For a proper evaluation of the behavior of this physical system it is vitally important to take into account "shake-off" and "shake-up" during photoionization. In contrast to the more common photoionization process, in which the final state consists of a single electron in the continuum and the remaining bound electrons in their initial configuration, "shake-off" results in two continuum electrons, and "shake-up" in a single continuum electron and an electron in an excited bound state. Of course, still higher-order processes are possible, and occur to some degree within the constraint of energy conservation. The importance of the second-order processes to the x-ray laser scheme being considered is readily seen. Considering boron in its neutral ground-state configuration of $1s^2 2s^2 2p$, shake-off during photoionization leads, for example, to the configuration

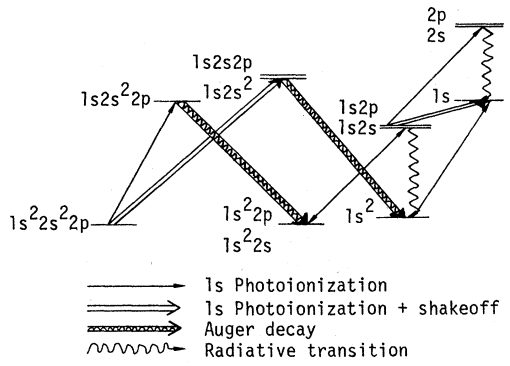

FIG. 1. Important atomic configurations and processes in multistage x-ray pumping of boron.

$1s2s^2$, which subsequently Auger decays to the configuration $1s^2$, which is the ground state of the prospective laser transition $1s2p \rightarrow 1s^2$, and leads by subsequent K-shell photoionization to the configuration $1s$, which is the ground state of the hydrogenic transition $2p \rightarrow 1s$. Figure 1 illustrates both the dominant pathway expected to produce inversion and the alternate pathways produced by Shake-off processes. Shake-off and shake-up rates are most often calculated in the "sudden" approximation,[4] and J. Scofield has kindly used his Hartree-Fock code to calculate the rates for the relevant boron configurations utilizing this approximation. The sudden approximation is expected to be valid except in cases where the photon energy is close to threshold,[4] in which case it overestimates the rate. The combined shake-off and shake-up fraction varies from 0.25 for the configuration $1s^22s^22p$ to the minimum value of 0.03 for the configuration $1s2s$, so it is quite significant.

The computer model is greatly simplified by considering all higher-order photoionization processes to result in shake-off, forgoing a detailed description of shake-up events and the large number of states such a description would entail. If one considers the fate of an electron which has been excited in a shake-up event, it is clear that the odds are overwhelming that it will rapidly find itself in the continuum. It is highly vulnerable to being shaken-off in any subsequent photoionization or Auger processes,[4] as well as to direct photoionization and collisional ionization. In contrast, radiative or collisional de-excitation are quite unlikely. During the time the electron remains bound in its excited state, its influence on the cross section for inner-shell processes is negligible, so the approximation used is expected to be a good one.

B. Resonance transitions

In addition to radiative transitions to the continuum, there are, of course, radiative transitions to a very large number of excited bound states. It is clear that the effect of such transitions must be considered carefully, since together they represent an oscillator strength greater than that for continuum absorption. Very many of these transitions have an unfavorable effect on the inversion, since they remove ions from the main pathway and frequently end up filling the laser ground state. For example, the radiative transition $1s^22s^22p \rightarrow 1s^22s^23s$ will result primarily in the filling of the $1s^2$ and $1s$ configurations, since as discussed above, the $3s$ electron is highly likely to rapidly find its way to the continuum in ensuing photoionizations, Auger processes, and collisions. Fortunately, however, even a small system such as we are considering here can have a great optical depth in the center of the resonance lines, so that the rate of upward resonance transitions is greatly reduced near the center of the system. Continuing with the example of the transition $1s^22s^22p \rightarrow 1s^22s^23s$, the wavelength of the transition is $\lambda = 2500$ Å, so that the peak cross section is $\sigma = \lambda^2/2\pi = 1.0\times10^{-10}$ cm^2. As will be discussed in detail in Sec. IV, the characteristic atom density is $n \approx 10^{19}$ and radial dimension $r \approx 10^{-3}$ cm for a practical x-ray laser experiment. This gives for the optical depth at line center $\tau \approx n\sigma r \approx 10^6$, so that the system is indeed very thick to line radiation. It must be pointed out that for the transition in question the spontaneous lifetime is $\tau_{spon} \approx 3\times10^{-9}$ sec, while the characteristic time scale for x-ray laser operation is $\tau_{xrl} \approx 10^{-12}$ sec. This indicates that photons absorbed by such a resonance transition cannot be reradiated during the time scale of interest, so that instead of the usual resonant scattering process which occurs in line transport, there is pure absorption.

Actually, it is necessary to be more careful, since the argument is correct only when the radiation field is very weak, so that stimulated emission can be neglected. For photon energies substantially below 1 keV, the photon flux necessary to produce inversion is approximately that of a 1-keV blackbody (see Sec. III). The characteristic time for reradiation of a photon in this radiation field must be reduced by the factor

$$\frac{1}{e^{h\omega/kT}-1} \approx \frac{kT}{h\omega},$$

which is the number of photons per mode—about 200 for the case of interest. This gives $\tau_s \approx 1.5\times10^{-11}$ sec which is still long compared to τ_{xrl}, so that the line indeed behaves as a pure absorber.

In this case, significant photon transport can occur to the center of the system only if the incident radiation flux is high enough to "burn through" the line by saturation. It is straightforward to show that this cannot happen in the situation being considered: The photon flux at frequency v in a (blackbody) cavity of temperature T is

$$F = \frac{8\pi v^2}{C^2} \frac{\Delta v}{e^{hv/kT} - 1}$$

$$\approx \frac{8\pi v^2}{C^2}\left(\frac{kT}{hv}\right) \Delta v \text{ photons/cm}^2 \text{ sec}$$

in a frequency band Δv wide. For the line under consideration, taking $\Delta v = 1/\tau_{spon}$ we have $F = 2.5_{21}$ photons/cm^2 sec. In a time $\tau_{xrl} = 10^{-12}$ sec this flux can saturate a maximum of $F\tau_{xrl}$ 2.5×10^{9} atoms/cm^2. On the other hand, we have $nr \approx 10^{19} \times 10^{-3} = 10^{16}$ atoms/cm^2, so that photons do not succeed in burning through.

The above argument that resonance transitions can be neglected is valid for all lines which have widths close to the natural width, although the numbers will vary somewhat from line to line. Transitions to states which are autoionizing, however, have linewidths much greater than natural, and the system is no longer highly opaque in these lines. Consider, for example, the transition $1s^22s^22p \rightarrow 1s2s^22p^2$. The upper state Auger decays to the configuration $1s^22s^2$, $1s^22s2p$, and $1s^22p^2$ with a rate which is not known directly, but may be bracketed with confidence by the KLL rates for boron and for carbon, to which it is isoelectronic. Using the KLL Auger rates of Walters and Bhalla,[5] we can set the Auger decay time of the upper state as $\tau_A \approx 1.5_{-14}$ sec. On the other hand, the radiative lifetime is $\tau_R \approx 4.0_{-12}$ sec, and putting in the transition wavelength of 69 Å, the peak absorption cross section is approximately

$$\sigma = \frac{\lambda^2}{2\pi}\frac{\tau_A}{\tau_R} = 2.8\times10^{-16} \text{ cm}^2 .$$

Using the same density and radial dimension as before, this results in an optical depth of only $nr\sigma \approx 2.8$. The situation is similar for all other transitions to autoionizing levels, particularly in the case of more highly ionized ground states, which never approach densities comparable to the total density, due to the transient nature of higher ionization stages. The computer model includes explicitly all resonance transitions to autoionizing levels and their subsequent Auger decay. The f values for all multiplets of these transitions have been calculated by Scofield,[6] and in calculating the transition rates the system is usually assumed to be thin in the lines, although any optical depth can be modeled.

C. Auger processes

The very rapid rate of Auger decays in low-Z elements makes possible two simplifying approximations in the computer model. The K-shell fluorescence yield of boron, neutral except for a single K-shell hole, is about 8×10^{-4}. The model assumes that the fluorescence yield for all autoionizing states is zero, so that no radiative decays of such states occur. This is a very good approximation, even for doubly excited states of helium-like boron. Additionally, Auger processes are assumed to occur instantaneously with respect to all other atomic processes, such as photoionization and collisional ionization. This assumption is occasionally marginal. For example, in the most intensely pumped cases discussed in Sec. III, the K-shell photoionization rate of neutral boron exceeds 10^{13} sec^{-1}, while the Auger decay rate is 5×10^{13} sec^{-1}. The error introduced at this level is not expected to be too serious, although extension of the model to still higher pumping fluxes would require the explicit inclusion of Auger rates in the rate equations.

In modeling the Auger decay of states excited by resonance transitions, it is important to note that the distribution of final states depends strongly on the spin and orbital angular momentum of the initial state. For example, some states, such as $2p^2(^3P)$, are forbidden to undergo Auger decay because of parity considerations, and in the absence of collisions will decay radiatively. In the model it is assumed that the multiplets of ground states are populated statistically, and that these states are radiatively excited into the various channels open to them at a rate proportional to the f value for each channel. The multiplets of the excited state then decay by KL_1L_1, KL_1L_{23}, and $KL_{23}L_{23}$ Auger processes in the same ratios as those calculated by Chen and Crasemann[7] for the same state of neon. The difference in Z between boron and neon is not expected to influence these ratios significantly. Angular momentum changing electron collisions are expected to be sufficiently rapid to destroy the metastability of states for which Auger decay is parity forbidden, but not rapid enough to affect states for which Auger decay is allowed.

Because of the relative emptiness of the L shell of boron, the double Auger process,[8] in which two electrons are ejected, is completely negligible. If higher-Z elements such as fluorine or neon were to be modeled, however, these processes would become significant.

D. Collisions

The successful operation of an x-ray laser as proposed here requires that the system be effec-

tively collisionless. If the rate of ionization due to electron collisions becomes significant compared to K-shell photoionization, no inversion will be produced because the loosely bound $2p$ electrons will be removed, and the upper laser state will not be filled. From this point of view, it is desirable to operate the system at as low a density as possible. On the other hand, one wishes to have as high a density as possible to increase the gain per unit length and reduce the required length of the system to a practical value.

An estimate of the density at which electron collisions begin to significantly degrade the performance of the system may be obtained quite simply: This occurs when $\tau_{\text{coll}} \equiv 1/n\sigma v \approx \tau_{\text{xrl}}$, where n is the electron density, σ is the average cross section for collisional ionization, and v is the average electron velocity, while τ_{xrl} is the characteristic time for the system to reach inversion, and is on the order of 10^{-12} sec. Collisional ionization cross sections for boron typically peak at an electron energy of about 100 eV, and have an average value of about $\pi a_0^2 = 9\times10^{-17}$ cm^2 in this region. If we use these values, $\tau_{\text{coll}} \approx \tau_{\text{xrl}}$ when $n \approx 2\times10^{19}$ cm^{-3}.

Because of the intense radiation flux, low density, and short times, the electron velocity distribution will not be Maxwellian, and an accurate calculation of the collisional rates would require solution of the time-dependent transport equation for the electrons. Fortunately, it is possible to show that such an approach is not necessary to obtain rates of accuracy consistent with the rest of the model. This is done by considering the collisional rates due to two limiting cases of the electron velocity distribution: The photoelectron distribution which would persist in the absence of collisions, and the Maxwell-Boltzmann distribution with the same energy which would result at high densities where electron-electron collisions enforce rapid thermalization. The photoelectron distribution is assumed to result from a blackbody radiation flux of temperature T_r incident upon atoms with a photoionization cross section given by

$$\sigma(E) = \sigma_{\text{th}}\left(\frac{E_{\text{th}}}{E}\right)^3 \quad E \geq E_{\text{th}},$$

$$= 0, \quad E < E_{\text{th}}.$$

This results in an electron velocity distribution (normalized to one) given by

$$f_{pe}(E)dE = \frac{dE}{A(E+E_{\text{th}})\left[e^{(E+E_{\text{th}})/kT_{r-1}}\right]},$$

where A is the normalization factor:

$$A = \int_{E_{\text{th}}/kT}^{\infty} \frac{du}{U(e^u-1)}.$$

This distribution is characterized by a long high-energy tail which is absent in a Maxwellian. The collisional ionization rate due to this distribution is obtained by integrating over a cross section of the form used by Lotz[9]:

$$\sigma_{ci}(E) = \sigma_{\max}\chi\frac{\ln(E/\chi)}{E}$$

where χ is the ionization potential. This gives the rate due to photoelectrons:

$$R_{pe} = n_e\int_0^{\infty} \sigma_{ci}(E) f_{pe}(E)\left(\frac{2E}{m}\right)^{1/2} dE.$$

This rate has been calculated numerically and compared with the rate due to a Maxwellian with the same energy R_{mb}. The ratio was found to be almost constant over the range of parameters found to be of interest for laser operation ($T_r/E_{\text{th}} \approx 3-5$, $E_{\text{th}}/\chi \approx 3-20$) and given approximately by $R_{pe}/R_{mb} = 0.8$. Collisional ionization cross sections are generally known to only 20% accuracy, and in view of the weak dependence of the ionization rate on the degree of thermalization, a detailed calculation of the electron velocity distribution is not warranted. Therefore, we have used the Maxwellian rates tabulated by Lotz[9] for ground state ions, and the expression of Seaton[10] for excited ions. A temperature of 160 eV has been assumed, which results from the thermalization of the photoelectrons produced by a 700-eV Planckian distribution incident upon atoms with K edge at 200 eV. The rates are not strong functions of temperature in this region and the choice of temperature is not critical.

The effect of electron collisions which change the angular momentum of excited states, already mentioned in connection with Auger decay of metastable states, has also been included in the code for heliumlike and hydrogenlike ions. While the peak cross section for these processes is extremely large, the electron distribution is far too hot to couple efficiently, and the rates are greatly reduced from their values at low temperatures. The cross sections of Sampson and Parks[11] have been used, and, as in the case of collisional ionization, calculated for both the photoelectron distribution and for the equivalent Maxwellian. The rate due to photoelectrons is calculated to be about 50% less than the rate due to the equivalent Maxwellian for the temperatures of interest. The rate for the fastest process (hydrogenic $2S \rightarrow 2p$) is about 2 psec^{-1} at an electron density of 10^{19}. Code calculations have shown that at an ion density of 10^{19}, which results in an electron density of 5×10^{19} when the system is fully ionized, the populations of the various angular momentum states are kept close to statistical equilibrium by collisions. At low densities these populations reflect the Auger branching ratio of the $1s2s^22p$ state,

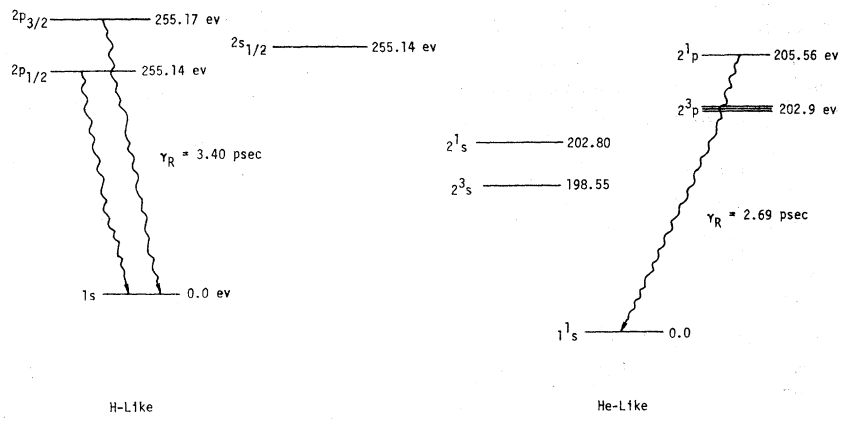

FIG. 2. Energy levels and radiative transitions for hydrogenlike and heliumlike boron ions.

which results in $1s^2 2p$ twice as often as $1s^2 2s^5$, so that the populations of hydrogen- and heliumlike p-states are underpopulated relative to their statistical values. This situation taken by itself makes high densities more favorable for the production of inversions, since the effect of angular momentum-changing collisions is to increase the population of the radiating p states at the expense of the nonradiating s states. However, since the rate of these collisions is not much greater than the rate of collisional ionization, this effect turns out to be quite small.

All other collisional processes, such as collisional and radiative recombinations, and collisional deexcitation, occur at negligible rates for the temperatures and densities of interest, and their inclusion in the code is not required.

E. Calculation of laser gain

In calculating the laser gain, heliumlike and hydrogenlike ions must be treated separately due to their different state structure and the different line-broadening mechanisms which are dominant in the two cases. The relevant states for the two ions are shown in Fig. 2. Considering the heliumlike ion first, only the 2^1P state has an allowed radiative transition to the 1^1S ground state. The $2^3P \rightarrow 1^1S$ intercombination transition occurs at a negligible rate (4.2×10^6 sec^{-1}) and is neglected here. The inversion density is

$$N^* = N_2 - (g_2/g_1)N_1,$$

where N_2 is the density of ions in the upper state, N_1 the density in the lower state, and g_2, g_1 are the degeneracies of the two states. In the case of a heliumlike ion, this becomes $N^*_{\mathrm{He}} = N_{2^1P} - 3N_{1^1S}$.

At relatively high densities, as discussed in Sec. II D, the multiplets of He-like ions remain in statistical equilibrium, so that $N_{2^1P} = \frac{1}{4}N_{1s2p}$, where N_{1S2P} is the total density of excited heliumlike ions in the $1s2p$ configuration. To have laser gain on the $2^1P \rightarrow 1^1S$ transition it is therefore necessary that $N_{1s2p} > 12N_{1s^2}$. At lower densities the requirement is more stringent since the 2^1P state has a smaller fraction of the total $1s2p$ population, due to its less than statistical rate of production and to its radiative decay. The situation is simpler for the hydrogenlike ion, where the inversion density is given by $N^*_{\mathrm{H}} = N_{2p} - 3N_{1s}$. Clearly, solely on the grounds of the state degeneracies, it is considerably more difficult to achieve inversion of heliumlike ions.

The linewidths expected for heliumlike and hydrogenlike transitions differ considerably as a result of the absence of the linear Stark effect in heliumlike systems. The contributions to the linewidth from the possible broadening mechanisms are listed in Table I for both helium- and hydrogenlike ions. The ion density is assumed to be 10^{19}, the electron temperature 150 eV, and the ion temperature 1 eV. The reason for the low-ion temperature, which makes the Doppler width negligibly small, is the slow rate of energy transfer from the electrons to the ions. The equilibration time[12] under these conditions is about 10^{-9} sec, three orders of magnitude greater than the time-scale of interest. It can be seen from Table I that for hydrogenlike ions, the linewidth is dominated by linear Stark broadening, while for heliumlike ions electron impact broadening is dominant, resulting in a linewidth twenty times smaller.

The laser gain at line center for a homogeneously broadened line is:

$$\alpha = N^*(\lambda^2/2\pi)\tau_{\mathrm{rad}}/\Gamma_{\mathrm{tot}},$$

where N^* is the inversion density, λ the transition wavelength, Γ_{rad} the radiative width, and τ_{tot} the

TABLE I. Contributions of various line-broadening mechanisms to the linewidths of H-like and He-like boron ions; $T_e = 150$ eV, $T_i = 1$ eV, $N_e = 5N_i = 5\times10^{19}$.

Broadening mechanism	H-like linewidth (eV)	He-like linewidth (eV)
Natural	2.6×10^{-4}	2.4×10^{-4}
Doppler	6.0×10^{-3}	4.8×10^{-3}
Fine structure	2.8×10^{-2}	...
Electron impact	$3.9\times10^{-3}(N_e/5\times10^{19})$	$6.0\times10^{-3}(N_e/5\times10^{19})$
Stark	$1.4\times10^{-1}(N_i/10^{19})^{2/3}$	...

total width. It is instructive to compute the gain for an inversion of 1% ($N^* = 0.01\ N$). Utilizing the values in Table I, the result is

$$\alpha_0^{\mathrm{H}} = 70(N/10^{19})^{1/3}\ \mathrm{cm}^{-1},\quad \alpha_0^{\mathrm{He}} = 1900\ \mathrm{cm}^{-1}.$$

The difference in density dependence reflects the difference in the line-broadening mechanisms.

III. RESULTS

The first question that the simulation code has been used to address is what photon flux is necessary to achieve inversion. Figure 3 shows the He-like and H-like inversions which result from an instantaneously turned on Planckian distribution as a function of the radiation temperature which characterizes the Planckian distribution. Two cases are illustrated: In one case, all photons below the 200-eV K edge of neutral boron have been removed, while in the second case the Planckian is unfiltered. In both cases zero density has been assumed so that electron collisions have no effect. Two facts are immediately appar-

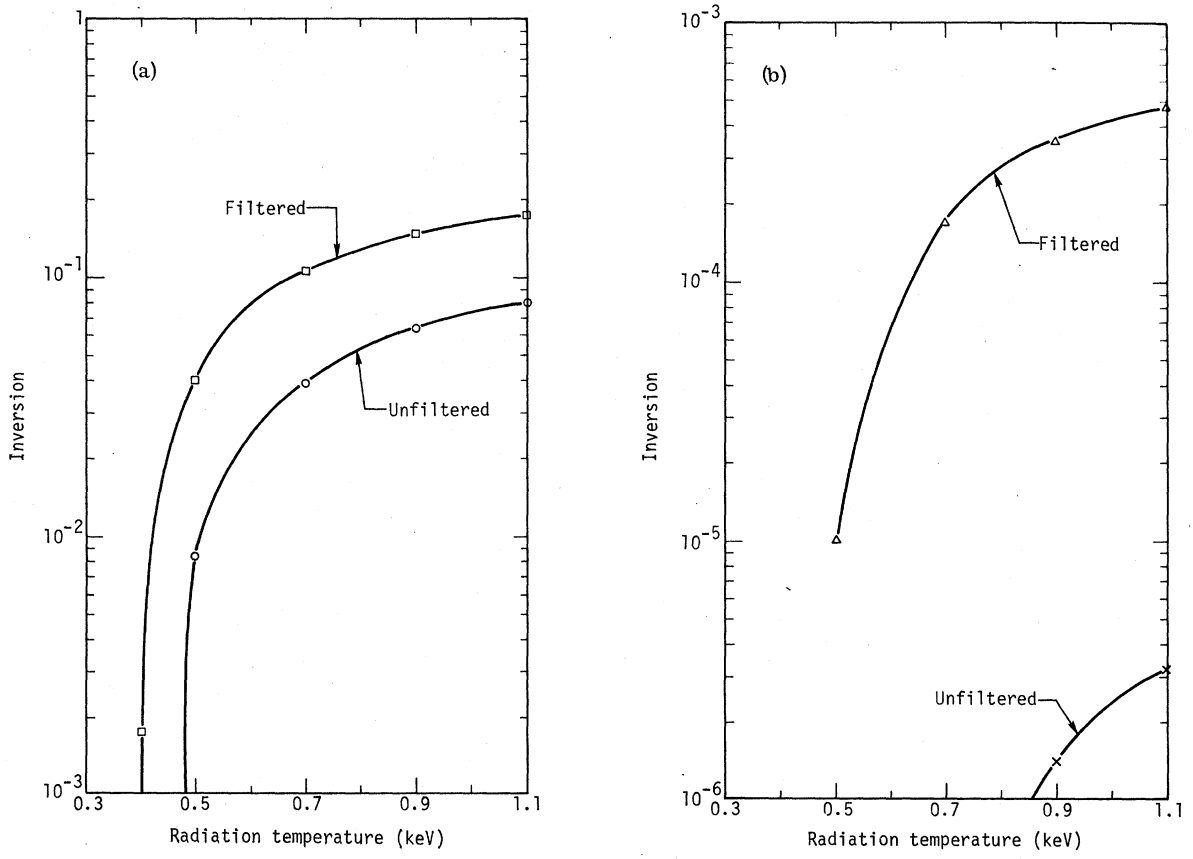

FIG. 3. Inversions due to filtered and unfiltered black-body sources. Inversions expressed as fraction of total population; (a) hydrogenlike, (b) heliumlike.

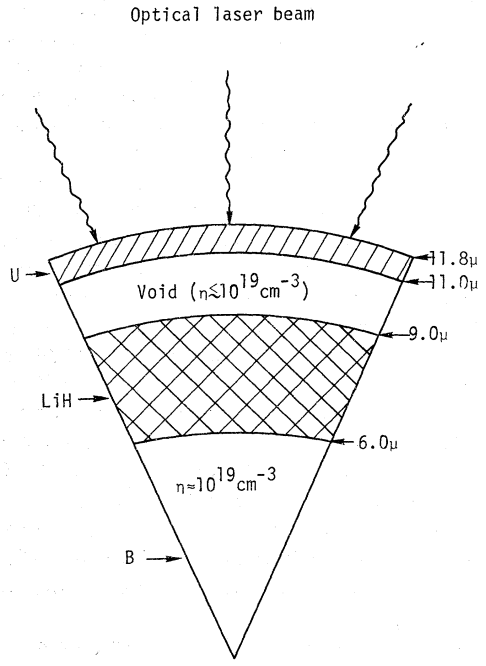

FIG. 4. Geometry and composition of model x-ray laser.

ent: A radiation temperature of about 500 eV is necessary to achieve significant H-like inversions; and that He-like inversions do not occur to any significant degree for any situation considered. It is clearly desirable to filter out the low energy photons, since their dominant effect is to produce L-shell ionizations which reduce the inversion. The effectiveness of filtering is particularly strong at low-radiation temperatures.

This information makes it possible to consider a somewhat more realistic situation. A schematic x-ray laser design is illustrated in Fig. 4, in which an intense optical laser beam heats a radiator, producing the pumping x-ray flux which passes through a filter on its way to the center region, which contains low density boron and constitutes the active region of the x-ray laser (XRL). Only a small fraction of the energy radiated by a 500-eV blackbody is effective in pumping the x-ray laser, namely, those photons between 200 eV and roughly 600 eV, and one might hope to reduce the intensity required of the pump laser by choosing a radiator material which emphasizes the effective part of the spectrum, and does not radiate effectively in the high energy part of the spectrum which contains most of the energy of the Planckian. This can be achieved by picking a low-Z material for the radiator, since the ratio of high frequency (1 keV) to low frequency (0.2 keV) opacity falls as Z is decreased. Unfortunately, due to the short time scale associated with inversion production ($\tau_{xrl} \approx 10^{-12}$ sec), a significant fraction of the pump laser power must be used simply to supply the internal energy of the radiator in the required time. In fact, we have found that for a high-Z radiator such as uranium, the amount of pump laser power necessary to supply internal energy and that needed to balance radiative loss are roughly equal. As Z is lowered, the internal energy requirement rapidly becomes dominant, and the total pump laser power required increases rapidly, in spite of the fact that the spectrum radiated is a more efficient one. Accordingly, a uranium radiator is used for the model XRL under discussion. Since the function of the filter is to remove photons of energy less than the 200 eV K edge of neutral boron while passing higher energy photons to the greatest extent possible, the choice of materials for its construction is limited mainly to the elements hydrogen through beryllium, although inclusion of small amounts of slightly higher-Z elements is a possibility. We have found that LiH is a nearly ideal filter material, and it is used for the model XRL.

Calculation of the performance of a model XRL is done in two steps. First LASNEX, a simulation code developed for laser fusion,[13] is used to model deposition of the pump laser energy, and subsequent radiation transport, electron conduction, and hydrodynamics. The time history of the radiation field in the central region, which contains the active XRL medium, is then used as the input to the simulation code described in the previous sections of this paper. For purposes of discussion here, the problem has been simplified somewhat by replacing the detailed LASNEX modeling of the laser energy deposition by an energy source in the radiator region which produces the desired radiator electron temperature, and by eliminating hydrodynamic motion.

To achieve a strongly inverted laser, a radiator electron temperature of 700 eV has been used, which is reached in 0.1 psec. Figure 5 illustrates the radiation spectrum present in the center of the problem after 1 psec and compares it to the same problem run without a filter. In Figure 6, the fractional populations of the most important states, and the H-like and He-like inversions are shown as functions of time. The ion density has been assumed to be low enough that the system is collisionless. Figure 7 illustrates the time dependence of the photoionization rates for the neutral and excited He-like ions. The increase of the rates with time reflects the temperature increase and accompanying drop in opacity of the filter due to both absorption of radiation and electron conduction from the radiator.

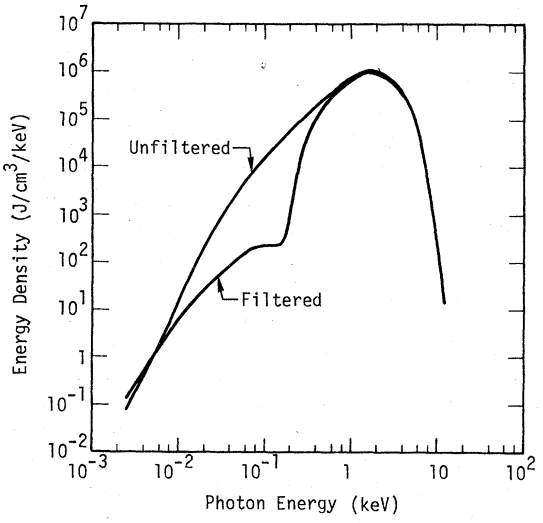

FIG. 5. Radiation spectrum at the center of the model x-ray laser of Fig. 4, 1 psec after turn-on of the energy source. Spectrum of same model without LiH filter is shown for comparison.

As shown in Fig. 6, the inversion initially becomes strongly negative, indicating resonant absorption, before it becomes positive. This is due almost exclusively to the shakeoff process during photoionization, which results in filling of the $1s$ ground state by processes such as $1s^2 2s^2 2p \rightarrow 1s 2s 2p \rightarrow 1s^2 \rightarrow 1s$, which involves only two photoionizations. The filling of the $2p$ upper state, which occurs by the process $1s^2 2s^2 2p \rightarrow 1s 2s^2 2p \rightarrow 1s^2 2p \rightarrow 1s 2p \rightarrow 2p$, requires three photoionizations, and takes longer. The inversion peaks approximately 1.5 psec after the onset of the pumping x-ray pulse, and its lifetime is determined by the 2.55 psec radiative lifetime of the $2p$ state, since the $2p$ photoionization rate is negligible in comparison.

It is worth noting that the 14% peak inversion attained in this problem actually exceeds the 11% attained by a 700-eV blackbody filtered below 200 eV, as shown in Fig. 3. This somewhat surprising result is due to the fact that the LiH filter reduces the intensity of the 248-eV radiation which excites the $1s 2p \rightarrow 2p^2$ resonance transition, and this effect outweighs the slight reduction of the K-shell ionization rates.

Figure 8 shows the dependence of the hydrogen-like gain on the atomic density. At low densities ($n < 10^{17}$ cm^{-3}) the fractional inversion is constant and the gain has the $n^{1/3}$ dependence given in the expression in Sec. II E. As the density increases, the fractional inversion increases slightly due to the effect of multiplet mixing collisions, and then rapidly decreases at densities greater than 10^{19} as collisional ionization destroys the inversion. The peak gain of 850 cm^{-1} is reached at a density of 1.2×10^{19}. The gain calculation assumes that losses can be ignored and this can readily be justified. Examination of Fig. 6 shows that at the time of peak inversion approximately 68% of the population consists of bare ions. The rest is made up of $1s$ (3%), $2s$ (7%), and $2p$ (22%) ions. The $1s$ ions do not absorb at the laser transition energy, while the $2s$ and $2p$ ions have absorption cross sections of approximately 5×10^{-20} cm^2 and 1×10^{-20} cm^2, respectively. At an atomic density of 10^{19}, this results in an absorption of 0.06 cm^{-1}, completely negligible compared with the 850 cm^{-1} gain. As a final point, it is of interest to check the effect of shake-off processes and resonance transitions on the gain. At a density of 10^{19}, if shake-off were not present the gain would be increased to 1400 cm^{-1}, while removal of resonance lines makes a small improvement to 890 cm^{-1}, a fact which reflects the effectiveness of the filter.

IV. DESIGN OF A PRACTICAL X-RAY LASER

The results of the previous section show that construction of an x-ray-pumped boron laser is at least possible in principle. The purpose of this section is to briefly discuss the technical problems which must be overcome before a successful experiment can be performed. One of the first questions which must be answered is whether the laser gain is high enough to permit simultaneous pumping of the laser over its entire length, or whether a swept excitation, as is currently used for some N_2 lasers,[14] is required. As discussed in Sec. III, the decay of the gain from its peak value is exponential, with time constant set by the radiative rate of the $2p \rightarrow 1s$ transition. In the case of simultaneous excitation, the gain-length product seen by a photon starting at one end of the laser at the time of peak inversion is given by

$$\int_0^L \alpha(x)dx = c \int_0^{L/c} \alpha_0 e^{-t/\tau} dt$$

$$= \alpha_0 c\tau (1 - e^{-L/c\tau}),$$

where α_0 is the peak gain, L is the laser length, τ is the radiative lifetime, and c is the speed of light. For the model XRL discussed in Sec. III, $\alpha_0 = 850$ cm^{-1}, $\tau = 0.765$ mm, and if we consider a 1-mm length, we find that

$$\int_0^L \alpha(x)\, dx = 47 .$$

This is generally considered to be more than adequate for obtaining reliable lasing in a mirrorless laser system. Unfortunately, as one con-

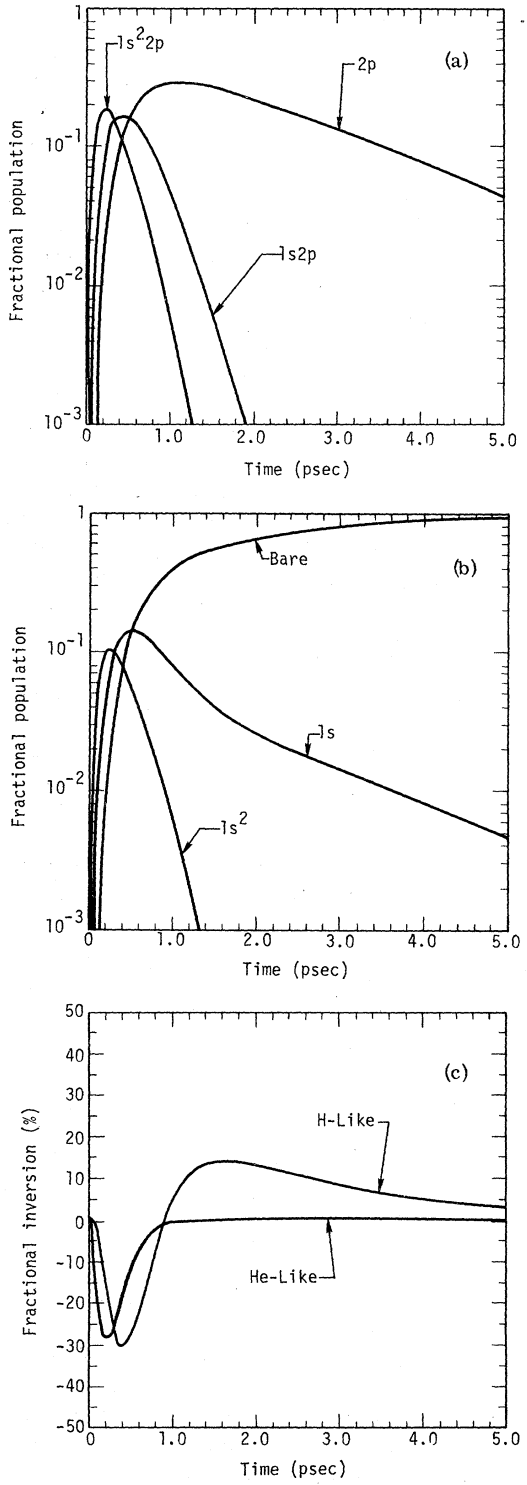

FIG. 6. Time history of population present in important atomic configurations, and of the hydrogenlike and heliumlike inversions for the model x-ray laser of Fig. 4. The ion density is low enough that the system is collisionless. All populations are expressed as fractions of the total.

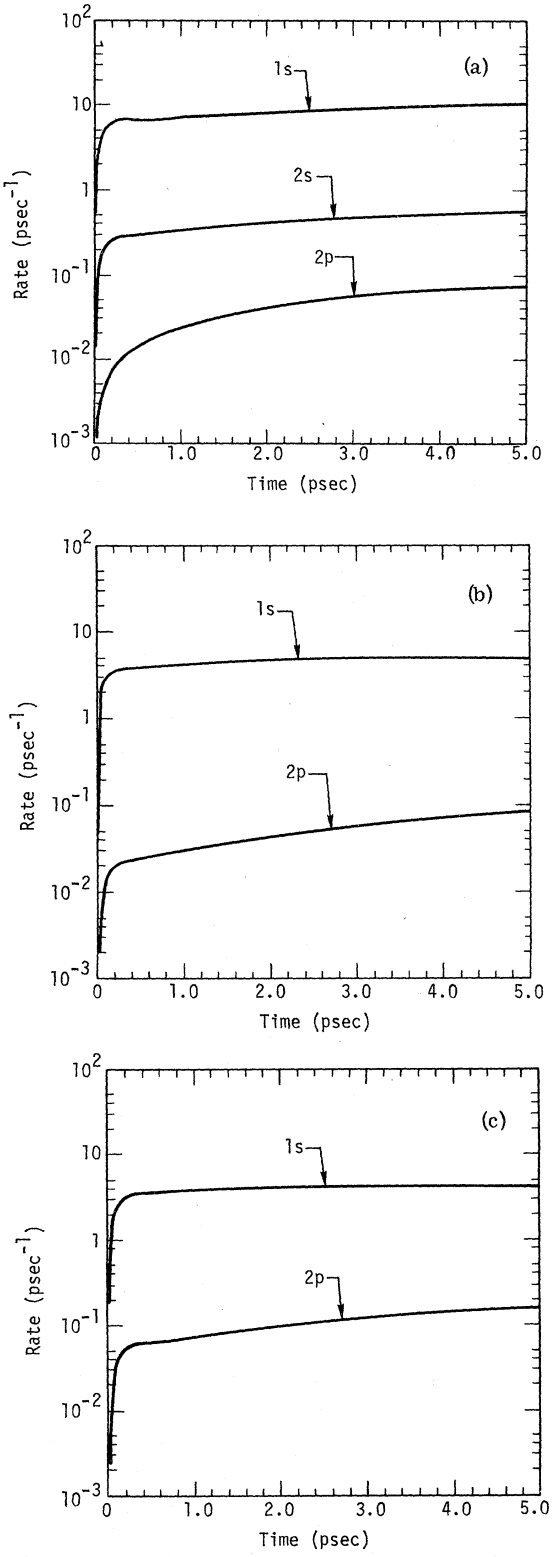

FIG. 7. Time history of the photoionization rates for the same situation as in Fig. 6. Rates are in $psec^{-1}$. (a) $1s^2 2s^2 2p$, (b) $1s2p$, (c) $1s$ and $2p$.

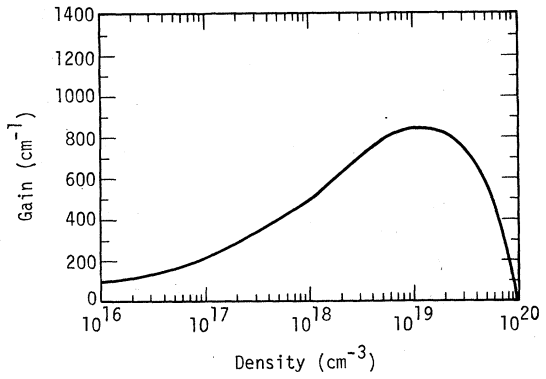

FIG. 8. Peak laser gain for hydrogenlike transition as a function of atomic boron density for the model x-ray laser of Fig. 4. Gain is in cm^{-1}.

siders more realistic XRL target designs this figure tends to deteriorate. In particular, the rise times of large glass laser systems are unlikely to become shorter than 5 psec, whereas the calculations of Sec. III assumed a risetime of 0.1 psec. Use of a 5-psec risetime reduces the peak gain by about a factor of 2. Hydrodynamic motion increases in importance as the rise time is lengthened, and causes further loss of gain due to expansion of the radiator. These effects make the system quite marginal for simultaneous excitation, and it is necessary to consider the possibility of swept excitation.

Swept excitation has several advantages. Since the pumping excitation travels at c, the laser length is no longer limited to the order of $c\tau$, and as high a gain-length product may be achieved as desired. As Hopf *et al.*,[15,16] have pointed out, however, the behavior of such a system may be quite anomalous, and the gain-length product no longer has the same meaning as for a simultaneously excited system and this will have to be considered carefully in the design of an experiment. Additionally, the power required of the pump laser is reduced, since it is no longer necessary to excite the entire length simultaneously, but only a length $c\tau_{inv}$, where τ_{inv} is the time required to reach peak inversion. For the example studied above, $c\tau_{inv} = 0.45$ mm, which is roughly half of the required length of the simultaneously excited system, thereby reducing the required power by a factor of two. A final advantage, which may be a decisive one, is that the rise time of the pump laser is no longer of great importance. One may imagine triggering the pump laser and waiting until it has come up to full power to begin the sweep along the XRL target. The time dependence of the pumping flux seen by a point on the XRL target is then governed by the spatial distribution of the intensiy in the focal spot of the pump laser as it moves by at velocity c. A rise time of 0.1 psec is generated in this manner by a focal spot with an intensity which rises from zero to maximum in a distance $\Delta x = c \times 10^{-13}$ sec $= 30\ \mu$, a seemingly achievable requirement. If a swept excitation is required to produce lasing, a major technological effort will be required to be able to sweep the high-power beam with the spatial and temporal precision required.

Successful operation of the model XRL considered here will require very great laser power. A 700-eV blackbody radiates a power of 2.5×10^{16} W/cm^2, and, as discussed earlier, a roughly equal power is required to supply the radiator internal energy in the required time, so that the laser must supply at least 5×10^{16} W/cm^2 to the target. The smallest practical target diameter is set by the pump laser focal spot size, which at present is certainly no smaller than 20μ. Assuming a swept system, the required laser power is roughly $P = 5 \times 10^{16} \times \pi \times 20\mu \times c\tau_{inv} = 1.4 \times 10^{13}$ W. Detailed calculations have shown it will be difficult to avoid exceeding this estimate by less than a factor of two, so that the laser-power requirements will tax the abilities of even the largest laser fusion lasers presently under construction, which are designed to produce about 2×10^{13} W. The power calculation assumes that all incident laser light is absorbed by the target, which certainly will not be the case. The reflection coefficient at such high laser intensities is largely unknown, and its measurement will be a crucial step in deciding whether an XRL as proposed here can become a practical reality.

A final problem, which has been discussed by Chapline,[3] is in what form the low-density boron is to be introduced into the XRL target. Boron melts at 2300 °C, which makes it difficult to use as atomic vapor, particularly in a target which contains LiH, which has a melting temperature of 690 °C. As Chapline has pointed out, use of a gaseous chemical compound such as diborane (B_2H_6), is unlikely to work due to the nature of the molecular dissociation which follows absorption of an x-ray photon and subsequent Auger decay. If this problem can be solved, it probably will be possible to perform experiments which check the validity of the x-ray laser simulation methods we have used, and possibly even to achieve lasing at soft x-ray energies.

ACKNOWLEDGMENT

The author would like to thank J. H. Scofield for calculation of the shake-off fractions and radiative rates used in the simulation code.

*Work performed under the auspices of the U. S. Energy Research and Development Administration, Contract No. W-7405-Eng-48.

[1]T. S. Axelrod, Phys. Rev. A 13, 376 (1976).
[2]F. T. Arecchi and G. P. Banfi, Opt. Commun. 10, 214 (1974).
[3]P. Hagelstein and G. Chapline, Appl. Phys. Lett. (to be published).
[4]T. Åberg, in *Proceedings of the International Conference on Inner Shell Ionization Phenomena and Future Applications*, edited by R. W. Fink, S. T. Manson, J. M. Palms, and P. V. Rao, CONF-720 404 (Natl. Tech. Information Service, U. S. Dept. of Commerce, Springfield, Va., 1972).
[5]D. L. Walters and C. P. Bhalla, Atomic Data 3, 301 (1971).
[6]J. H. Scofield (private communication).
[7]M. H. Chen and B. Crasemann, Phys. Rev. A 12, 959 (1975).
[8]T. Åberg, in *Atomic Inner-Shell Processes*, edited by B. Crasemann (Academic, New York, 1975), Vol. 1.
[9]W. Lotz, Astrophys. J. Suppl. 14, 207 (1967).
[10]M. J. Seaton, in *Atomic and Molecular Processes*, edited by D. R. Bates (Academic, New York, 1962).
[11]D. H. Sampson and A. D. Parks, Astrophys. J. Suppl. 28, 323 (1974).
[12]L. Spitzer, *Physics of Fully Ionized Gases* (Interscience, New York, 1962).
[13]G. Zimmerman, Lawrence Livermore Laboratory Report No. UCRL-50021-72-1 (unpublished).
[14]H. Strohwald and H. Salzmann, Appl. Phys. Lett. 28, 272 (1976).
[15]F. Hopf and P. Meystre, Phys. Rev. A 12, 2534 (1975).
[16]R. Bonifacio, F. Hopf, P. Meystre, and M. Scully, Phys. Rev. A 12, 2568 (1975).